

**TECHNICAL EVALUATION OF THE KODAK DIRECTVIEW
MAMMOGRAPHY COMPUTERISED RADIOGRAPHY SYSTEM
USING EHR-M2 PLATES**

**NHSBSP Equipment Report 0706
May 2007**

**KC Young and JM Oduko
National Coordinating Centre for the Physics of Mammography**

Enquiries

Enquiries about this report should be addressed to:

Professor KC Young

National Coordinating Centre for the Physics of Mammography

Medical Physics Department

Royal Surrey County Hospital

Guildford

GU2 7XX

Tel: 01483 406738

Fax: 01483 406742

Email: ken.young@nhs.net

Published by

NHS Cancer Screening Programmes

Don Valley House

Savile Street

Sheffield

S4 7UQ

Tel: 0114 271 1060

Fax: 0114 271 1089

Email: info@cancerscreening.nhs.uk

Website: www.cancerscreening.nhs.uk

© NHS Cancer Screening Programmes 2007

The contents of this document may be copied for use by staff working in the public sector but may not be copied for any other purpose without prior permission from the NHS Cancer Screening Programmes.

The report is available in PDF format on the NHS Cancer Screening Programmes' website.

Typeset by Prepress Projects Ltd, Perth (www.prepress-projects.co.uk)

Printed by **TO BE CONFIRMED**

CONTENTS

	Page No
1. INTRODUCTION	1
1.1 Testing procedures and performance standards for digital mammography	1
1.2 Objectives	1
2. METHODS	1
2.1 System tested	1
2.2 Detector response and noise analysis	1
2.3 Dose measurement	2
2.4 Contrast to noise ratio	2
2.5 Image quality measurements	3
2.6 Optimisation	3
3. RESULTS	4
3.1 Detector response	4
3.2 Noise measurements	5
3.3 AEC performance	6
3.4 Image quality measurements	8
3.5 Comparison with other systems	10
3.6 Optimisation	13
4. DISCUSSION	15
5. CONCLUSIONS	15
REFERENCES	16

1. INTRODUCTION

1.1 Testing procedures and performance standards for digital mammography

This report is one of a series evaluating the technical performance of commercially available digital mammography systems on behalf of the NHS Breast Screening Programme (NHSBSP). The testing methods and standards applied in this report were mainly derived from NHSBSP Equipment Report 0604.¹ This is referred to in this document as the NHSBSP protocol and it has the same image quality and dose standards as those provided in the European protocol.^{2,3} The European protocol was followed where there is a more detailed performance standard, eg for the automatic exposure control (AEC) system.

1.2 Objectives

The purpose of these tests was to determine whether this system met the main standards in the NHSBSP and European protocols, and to provide performance data for comparing this system against other manufacturers' products. Additional measurements were also undertaken to assess how well the automatic exposure control was optimised. The method of assessing optimisation has been reported previously.^{4,5} A previous NHSBSP Report evaluated this manufacturer's CR system with the original image plate design (EHR-M).⁶ Clinical evaluations are published separately by the NHSBSP where systems meet the minimum standards in the NHSBSP protocol.

2. METHODS

2.1 System tested

The system tested is shown in Table 1. The tests were conducted at a private hospital on 6 November 2006. The difference from the previously tested system was the new design of image plate (EHR-M2) and an adjustment to the AEC to compensate. The AEC programme and density setting were chosen on the recommendation of the CR manufacturer.

Table 1 System tested

Model of CR reader	X-ray set	AEC settings	Cassette	Image plate	Pixel size (µm)
Kodak DirectView CR 850 (software version 4.5 with mammography upgrade)	GE Senographe DMR+	Standard mode, density = +3	CR mammography cassette	EHR-M2	50

2.2 Detector response and noise analysis

The detector response was measured broadly as described in the NHSBSP protocol. A phantom of polymethylmethacrylate (PMMA) with total thickness of 45 mm was positioned at the tube exit port and exposed using a tube voltage of 27 kV and a Mo/Rh target/filter combination. A CR cassette was placed on the breast support table with the bucky system removed. An ion chamber was positioned at the surface of the CR cassette and the entrance surface air kerma measured for a range of tube current-time products. The readings were corrected to the surface of the imaging cassette using the inverse square law. No correction was made for attenuation by the cover of the cassette. The images were saved as unprocessed files and transferred to another computer for analysis. A 10 mm square region of interest (ROI) was positioned on the mid-line and 6 cm from the chest wall

edge of each image and adjacent to the position of the ion chamber. The average pixel value and the standard deviation of pixel values within that region were measured. The relationship between average pixel values and the detector entrance surface air kerma was determined. The standard deviations for the pixel values in the ROI for each image were used to investigate the relationship between dose to the detector and image noise.

2.3 Dose measurement

Doses were measured by using the AEC to expose different thicknesses of PMMA to simulate breasts. U-shaped expanded polystyrene spacers were added to adjust the total thickness to be equal to the equivalent breast thickness. To measure the contrast to noise ratio (CNR) an aluminium square (10 mm × 10 mm) of 0.2 mm thickness was placed on top of the 20 mm thick block, with one edge on the midline and 6 cm from the chest wall edge. Additional layers of PMMA and spacers were added on top to vary the total thickness.

2.4 Contrast to noise ratio

The images of the blocks of PMMA obtained during the dose measurement were analysed to obtain the CNRs. Multiple small ROIs (< 3 mm × 3 mm) were used to determine the average signal and the standard deviations in the signal within the image of the aluminium square and the surrounding background. Small ROIs were used to minimise distortions due to the heel effect. CNR then was calculated for each image as defined in the NHSBSP and European protocols.

To apply the standards in the European protocol the limiting value for CNR (using 50 mm PMMA) was determined according to equation 1. This equation determines the CNR value ($CNR_{limiting\ value}$) that is necessary to achieve the minimum threshold gold thickness for the 0.1 mm detail (ie $threshold\ gold_{limiting\ value} = 1.68\ \mu m$ which is equivalent to $threshold\ contrast_{limiting\ value} = 23.0\%$ using 28 kV Mo/Mo). Threshold contrasts were calculated as described in the European protocol and used in equation 1.

$$Threshold\ contrast_{measured}\ CNR_{measured} = Threshold\ contrast_{limiting\ value}\ CNR_{limiting\ value} \quad (1)$$

The relative CNR was then calculated according to equation 2 and compared with the limiting values provided for relative CNR shown in Table 2. The minimum CNR required to meet this criterion was then calculated.

$$Relative\ CNR = CNR_{measured} / CNR_{limiting\ value} \quad (2)$$

Table 2 Limiting values for relative CNR

Thickness of PMMA (mm)	Equivalent breast thickness (mm)	European protocol limiting values for relative CNR (%)
20	21	> 115
30	32	> 110
40	45	> 105
45	53	> 103
50	60	> 100
60	75	> 95
70	90	> 90

2.5 Image quality measurements

Contrast detail measurements were made using the CDMAM phantom (version 3.4, UMC St Radboud, Nijmegen University, The Netherlands). The phantom was positioned with a 20 mm thickness of PMMA blocks above and below, to give a total attenuation approximately equivalent to 50 mm of PMMA or a 60 mm thickness of typical breast tissue. This arrangement was imaged using the x-ray set's automatically selected factors normally set for clinical use for a breast of equivalent attenuation, ie 60 mm thick. This procedure was repeated 15 times to obtain a representative sample of 16 images. (Using a large number of images increases the accuracy of the automated image quality measurements.) Unprocessed images were transferred to disk for subsequent analysis off-site. The digital images had their contrast and density adjusted to optimally display the details in the test object, before scoring on a DICOM calibrated monitor. These image quality measurements were then repeated using eight exposures at each of the two other dose levels by manually selecting higher and lower mAs values with the same beam quality as selected under AEC control.

For an image quality measurement at each dose level three observers reviewed four of the digital images on a soft copy display and the test object manufacturer's correction scheme was then applied, before determining the threshold gold thickness for each detail diameter.

The average threshold gold thickness for each detail diameter for each dose level (an average for four images and three experienced observers) was fitted with a curve as described in the NHSBSP protocol. The measured threshold gold thicknesses typically have 95% confidence limits of about 10%. The threshold contrasts quoted in the tables of results are derived from the fitted curves, as this has been found to improve the accuracy.⁶

The expected relationship between threshold contrast and dose was plotted with the experimental data and is given by equation 3.

$$\text{Threshold contrast} = \lambda D^{-n} \quad (3)$$

The appropriate value of n was determined from the analysis of the noise as a function of the pixel value. In practice this was done by finding the value of n that provided the best fit to the experimental data. D represents the mean glandular dose (MGD) for a 60 mm thick standard breast equivalent to the test phantom configuration used for the image quality measurement. λ is a constant to be fitted.

An automatic method of reading the CDMAM images was also used. This produces a prediction of the threshold gold thickness for a typical human observer using a method that has been described elsewhere.^{6,7} The main advantage of automatic reading is that it has the potential of eliminating observer error which is a significant problem when using human observers. However it should be noted that at the present time the official protocols still require human reading.

2.6 Optimisation

A method for determining optimal beam qualities and exposure factors for digital mammography systems has been described previously and was used to evaluate this system.^{4,5} CNR and mean glandular dose were measured as described above using blocks of PMMA from 20 to 70 mm thick. For each thickness up to five tube voltage settings were used (25, 28, 31, 34 and 37 kV) with each of the target/filter combinations available (Mo/Mo, Mo/Rh and Rh/Rh) and the mAs recorded. The MGDs to typical breasts with attenuation equivalent to each thickness of the PMMA were calculated as described in the NHSBSP protocol. Each exposure was designed to achieve a standard pixel value by using the AEC in automatic mAs mode. The relationship between noise and pixel values in digital mammography systems has been previously⁵ shown to be approximated by

$$\text{Relative noise} = \sqrt{\frac{sd(bgd)^2 + sd(Al)^2}{2p}} = k_i p^{-n} \quad (4)$$

where k_i is a constant, and p is the average background pixel value linearised with absorbed dose to the detector. The value of n was found by fitting this equation to the experimental data. Equation 5 was then used to calculate the dose required to achieve a target CNR, where k is a constant to be fitted

$$\text{CNR} = kD^n \quad (5)$$

The target CNR was that calculated to reach either the minimum or achievable image quality in the NHSBSP and European protocols using the following relationship.

$$\text{Threshold contrast} = \frac{\lambda}{\text{CNR}} \quad (6)$$

where λ is a constant that is independent of dose, beam quality and the thickness of attenuating material. The optimal beam quality for each thickness was selected as that necessary to achieve the target CNR for the minimum dose.

3. RESULTS

3.1 Detector response

The detector response measurements were made with the grid removed and at the surface of the cassette. No correction was made for attenuation by the cassette cover. The images were found to have a non-linear response as shown in Figure 1. The AEC typically selected exposures to achieve a pixel value of about 1100 ± 40 (SD) which corresponds to a mean detector entrance air kerma of $88.5 \mu\text{Gy}$. A curve fitted to the data in Figure 1 was used to linearise the pixel values with respect to dose absorbed by the detector for subsequent measurements as shown in Figure 2. A raw pixel value of 1100 was used to calculate the detector reference air kerma for a range of kV, filter and target material combinations as shown in Figure 3.

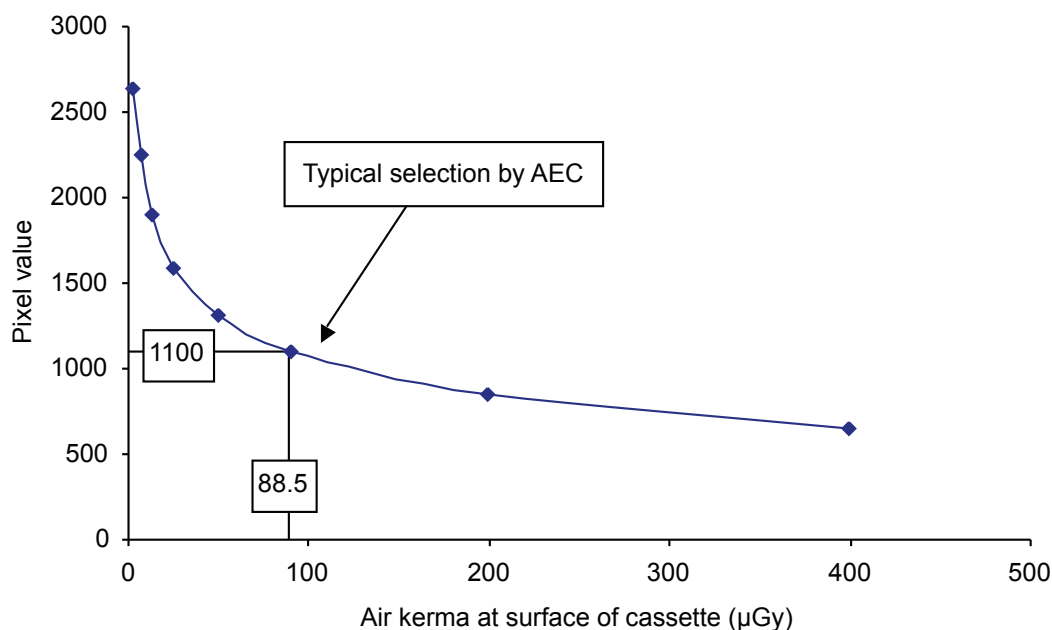


Figure 1 Detector response using 27 kV Mo/Rh.

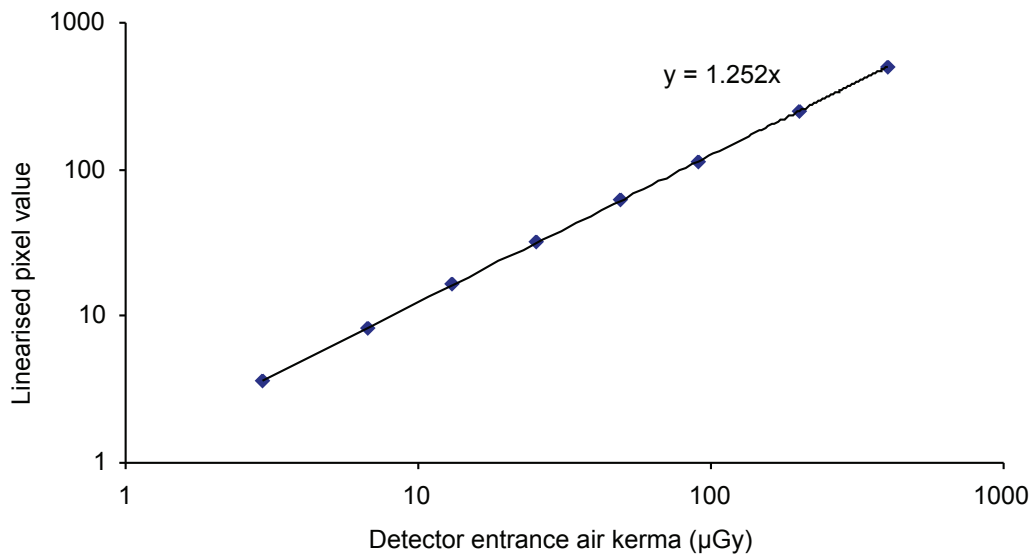


Figure 2 Linearised pixel values.

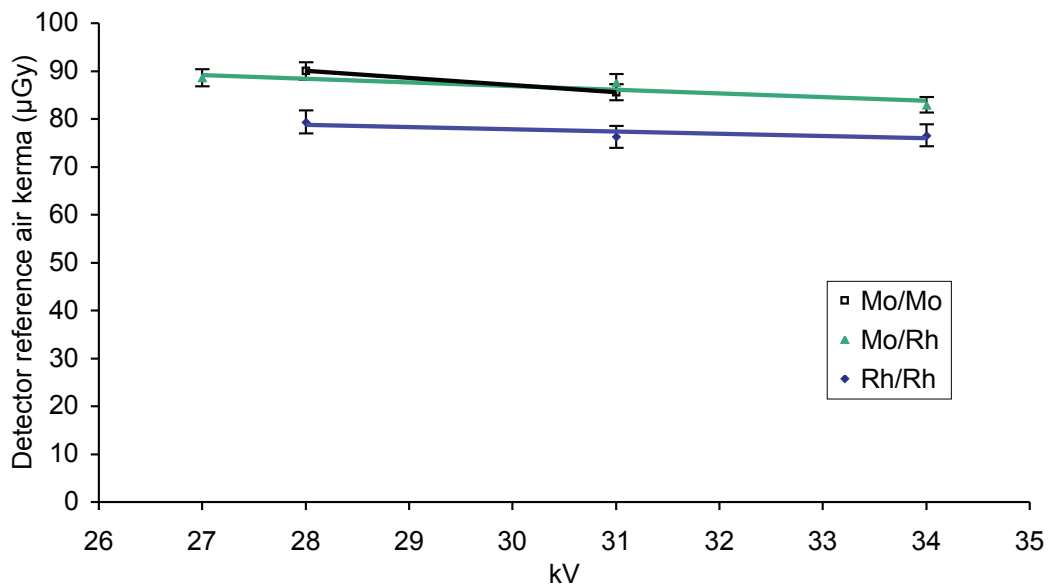


Figure 3 Detector reference air kerma for a raw pixel value of 1100.

3.2 Noise measurements

The variation in noise with dose was analysed by plotting the detector entrance air kerma against the standard deviation in linearised pixel values as shown in Figure 4. The fitted power curve has an index of 0.52. If only quantum noise sources were present the data would form a straight line with an index of 0.5. The presence of some electronic noise and structural noise has caused the curve to deviate from a straight line. This is normal for such systems and quantum noise was the dominant noise source.

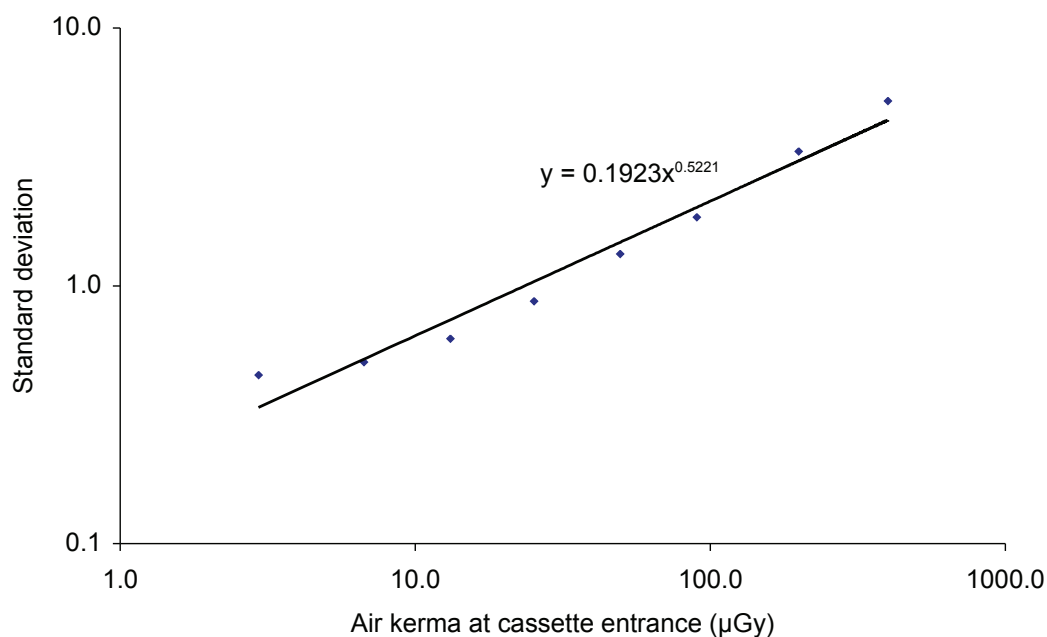


Figure 4 Standard deviation of pixel values versus detector entrance air kerma using 27 kV Mo/Rh.

3.3 AEC performance

3.3.1 Dose

The mean glandular doses for breasts simulated with PMMA exposed under AEC control in the Standard mode as set up for clinical use by the Kodak engineers are shown in Table 3 and Figure 5. At all thicknesses the dose was below the remedial level in the NHSBSP protocol which is the same as the maximum acceptable level in the European protocol.

Table 3 Mean glandular doses for simulated breasts

PMMA thickness (mm)	Equivalent breast thickness (mm)	kV	Target	Filter	mAs	MGD (mGy)	NHSBSP remedial level (mGy)
20	21	25	Mo	Mo	29	0.59	> 1.0
30	32	26	Mo	Mo	55	0.78	> 1.5
40	45	28	Mo	Mo	80	1.56	> 2.0
45	53	27	Mo	Rh	111	1.64	> 2.5
50	60	29	Mo	Rh	110	1.99	> 3.0
60	75	29	Rh	Rh	160	2.55	> 4.5
70	90	30	Rh	Rh	244	3.88	> 6.5

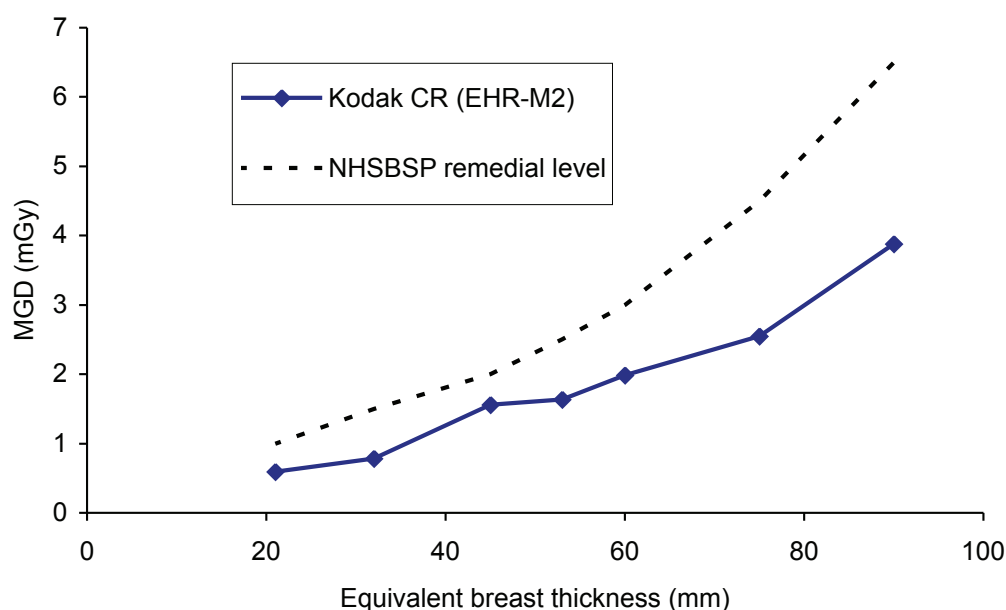


Figure 5 MGD for simulated breasts.

3.3.2 CNR

The results of the contrast and CNR measurements are shown in Table 4 and Figure 6. The CNR required to meet the minimum acceptable and achievable image quality standards at the 60 mm breast thickness have been calculated and are shown in Table 4 and Figure 6. The CNR values required at each thickness to meet the limiting values for CNR in the European protocol are also shown.

Table 4 Contrast and CNR measurements using AEC

Equivalent breast thickness (mm)	kV target filter	mAs	Background pixel value ^a	% contrast for 0.2 mm Al square	Measured CNR	CNR at minimum acceptable IQ	CNR at achievable IQ	CNR to meet European limiting value	EUREF limiting values for relative CNR
21	25 Mo/Mo	29	100	21.0%	13.1	8.28	12.05	9.52	> 115
32	26 Mo/Mo	55	105	19.3%	12.1	8.28	12.05	9.10	> 110
45	28 Mo/Mo	80	110	16.9%	10.7	8.28	12.05	8.69	> 105
53	27 Mo/Rh	111	113	15.3%	9.7	8.28	12.05	8.52	> 103
60	29 Mo/Rh	110	113	14.3%	8.8	8.28	12.05	8.28	> 100
75	29 Rh/Rh	160	132	12.3%	8.0	8.28	12.05	7.86	> 95
90	30 Rh/Rh	244	141	11.3%	7.5	8.28	12.05	7.45	> 90

a These background pixel values have been linearised with dose absorbed by the detector.

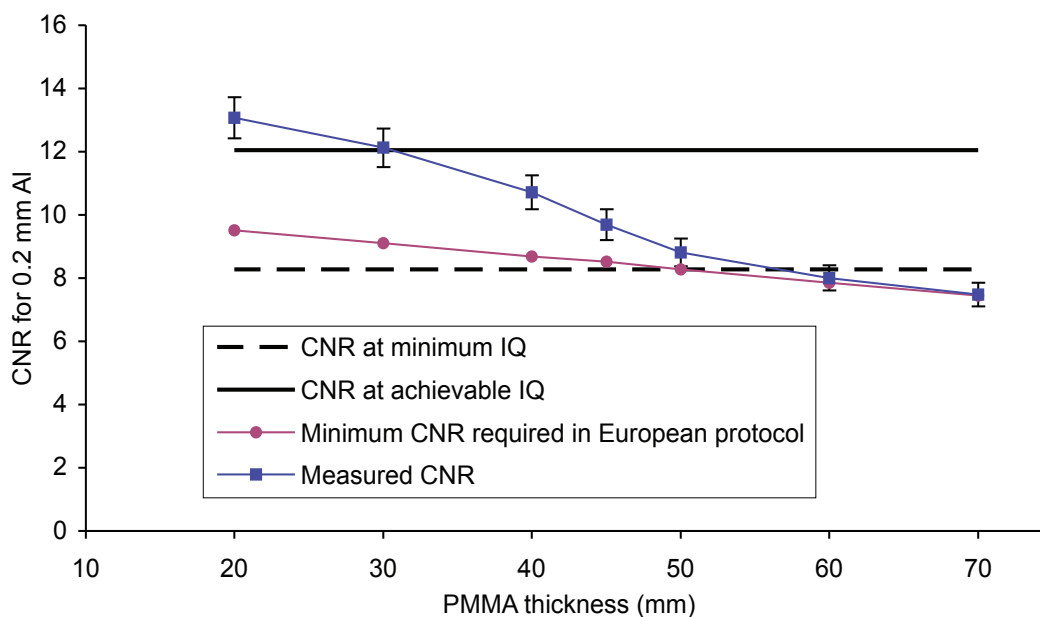


Figure 6 Measured CNR compared to the limiting values in the European protocol (error bars indicate 95% confidence limits).

3.4 Image quality measurements

The first exposures of the image quality phantom were made using the AEC to select the beam quality and exposure factors. This resulted in the selection of 27 kV Mo/Rh and 160 mAs and an MGD of 2.18 mGy to an equivalent breast. Subsequent image quality measurements were made at half and double this dose by manual selection of the mAs at the same beam quality. The threshold gold thicknesses for different diameters and the three different dose levels are shown in Table 5, along with the minimum and achievable threshold values from the NHSBSP protocol. The contrast detail curves at the three dose levels are shown for human and automatic reading in Figure 7a and b. The system meets the minimum acceptable standard for all doses except the lowest. The measured threshold gold thicknesses are plotted against the dose for the 0.1 and 0.25 mm detail sizes in Figure 8. This illustrates that when the dose was increased the threshold contrast reduced as expected by the theory. The fitted curves in Figure 8 were used to determine the doses required to meet the minimum acceptable and achievable image quality levels for comparison with other systems in the next section. In practice this is dictated by the threshold contrast for the 0.1 mm detail size as this requires the highest dose. Figure 8 also shows the predicted threshold gold thickness using automated reading at each dose level.

Table 5 Average threshold gold thicknesses for different detail diameters for three different doses using 27 kV Mo/Rh using human readers

Diameter (mm)	Threshold gold thickness (µm)				
	Acceptable value	Achievable value	MGD = 1.09 mGy	MGD = 2.18 mGy	MGD = 4.36 mGy
0.1	1.680	1.100	2.53	1.56	1.33
0.25	0.352	0.244	0.41	0.29	0.20
0.5	0.150	0.103	0.17	0.12	0.10
1	0.091	0.056	0.086	0.065	0.058
2	0.069	0.038	0.049	0.047	0.042

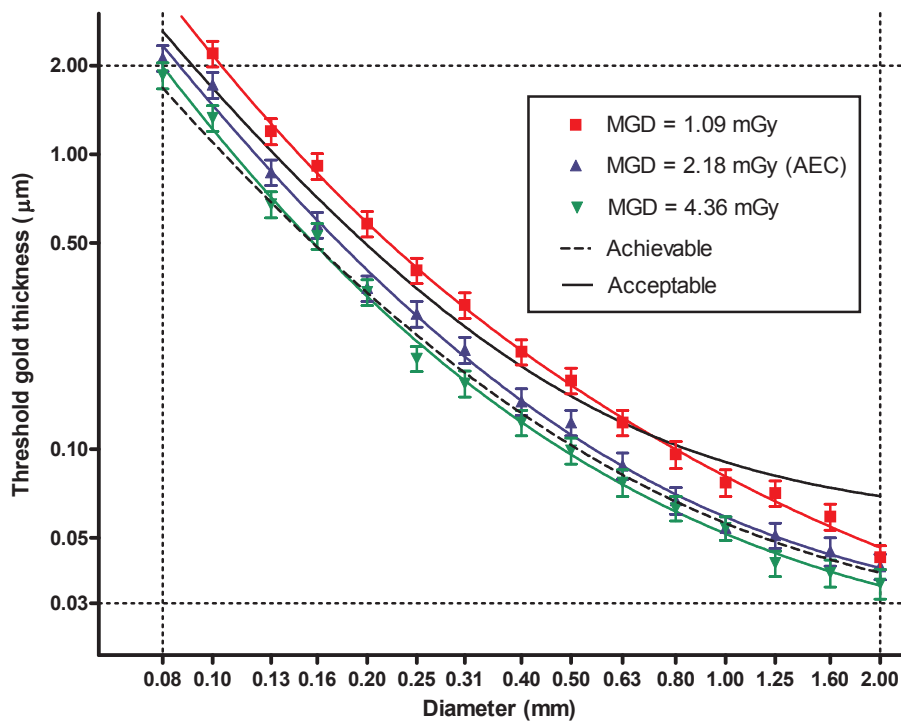


Figure 7a Contrast–detail curves for three different doses at 27 kV Mo/Rh using human readers. The straight dashed lines indicate the minimum and maximum detail diameters and gold thicknesses within the test object.

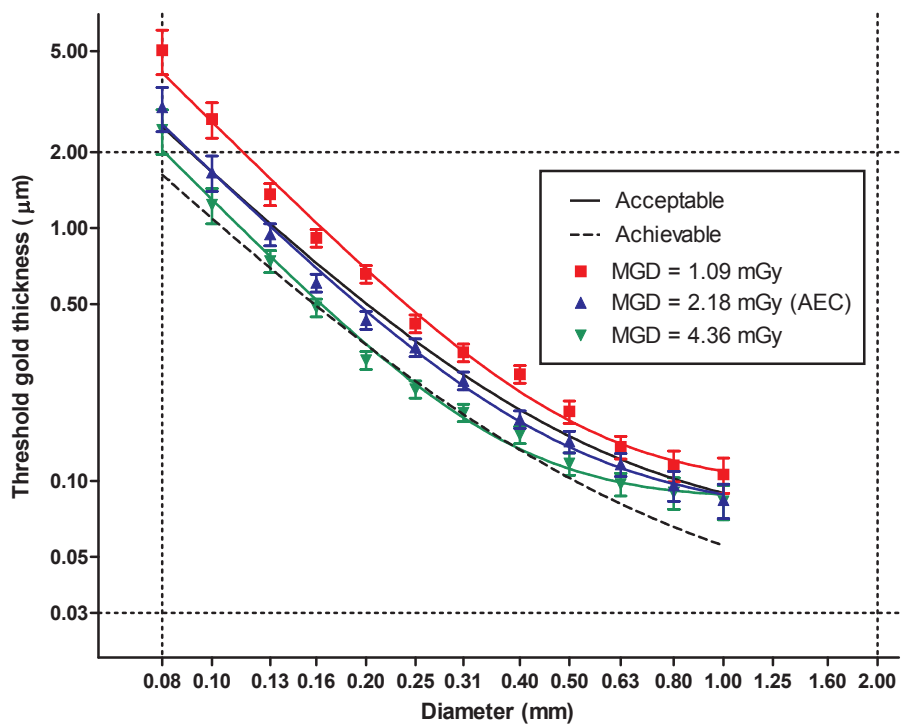


Figure 7b Contrast–detail curves for three different doses at 27 kV Mo/Rh using results predicted from automatic reading. The straight dashed lines indicate the minimum and maximum detail diameters and gold thicknesses within the test object.

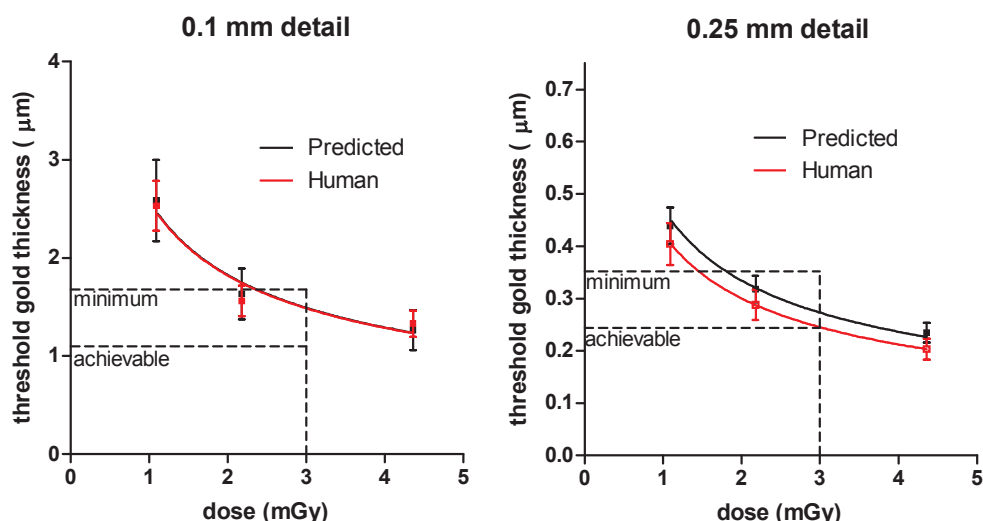


Figure 8 Threshold gold thickness at different doses.

3.5 Comparison with other systems

The MGDs to reach the minimum and achievable image quality standards in the NHSBSP protocol have been estimated from the curves shown in Figure 8. (The error in estimating these doses depends on the accuracy of the curve fitting procedure, and pooled data for several systems have been used here to estimate the 95% confidence limits of about 20%.) These doses are shown against similar data for other digital mammography systems in Tables 6 and 7 and Figures 9–12. The data for the other systems have been determined in the same way as described in this report and the results published previously.⁶⁻⁸ The data for film screens represent an average value determined using a variety of film screen systems.

Table 6 The MGD for different systems to reach the minimum threshold gold thickness for 0.1 and 0.25 mm details

System	MGD (mGy) for 0.1 mm		MGD (mGy) for 0.25 mm	
	Human	Predicted	Human	Predicted
Fischer Senoscan	0.55	0.42	0.48	0.53
Sectra MDM	0.60	0.82	0.67	0.46
Siemens Novation	0.63	0.61	0.52	0.63
Hologic Selenia	0.85	0.55	0.80	0.53
GE DS	1.01	0.82	0.87	0.83
Film-screen	1.17	1.30	1.07	1.36
Fuji Profect CR	1.67	1.78	1.45	1.35
Kodak CR (EHR-M)	3.46	2.49	1.49	1.33
Kodak CR (EHR-M2)	2.29	2.34	1.45	1.80
Test CR	4.52	4.17	2.33	2.12

Technical Evaluation of the Kodak DirectView Mammography CR System

Table 7 The MGD for different systems to reach the achievable threshold gold thickness for 0.1 and 0.25 mm details

System	MGD (mGy) for 0.1 mm		MGD (mGy) for 0.25 mm	
	Human	Predicted	Human	Predicted
Fischer Senoscan	1.16	0.90	0.98	1.09
Sectra MDM	1.27	1.74	1.37	0.95
Siemens Novation	1.56	1.21	1.14	1.27
Hologic Selenia	1.84	1.19	1.685	1.12
GE DS	2.35	1.57	1.80	1.87
Film-screen	2.48	3.03	2.19	2.83
Fuji Profect CR	4.26	3.29	3.52	2.65
Kodak CR (EHR-M)	7.74	5.56	6.28	5.60
Kodak CR (EHR-M2)	5.34	5.45	3.03	3.74
Test CR	11.5	9.90	5.96	5.63

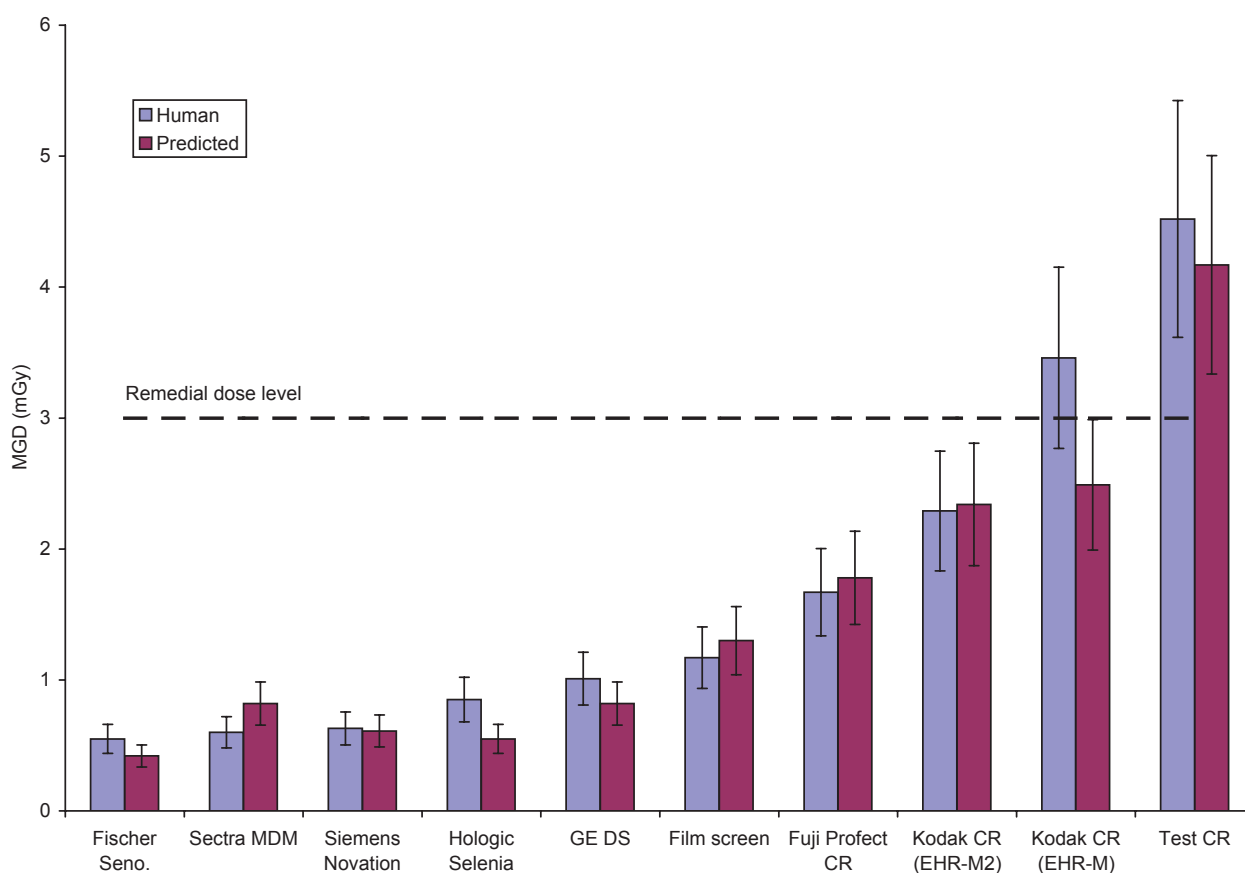


Figure 9 Dose to achieve minimum acceptable image quality standard for 0.1 mm detail (error bars indicate 95% confidence limits).

Technical Evaluation of the Kodak DirectView Mammography CR System

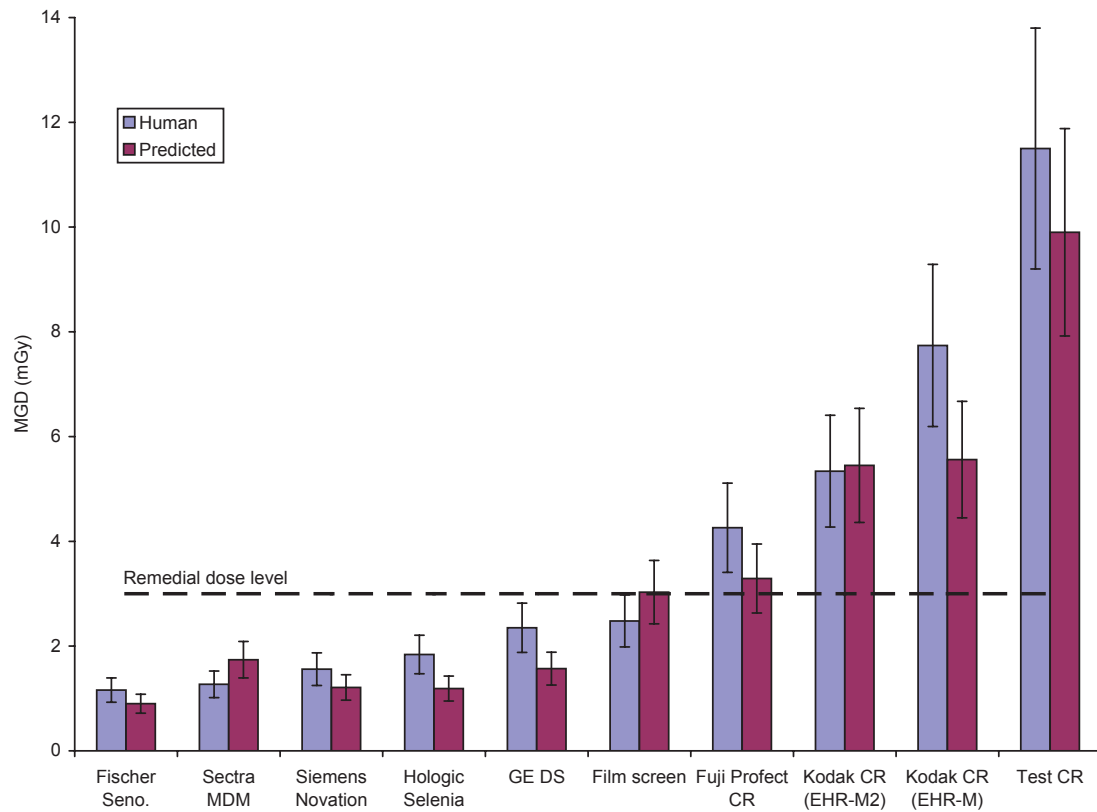


Figure 10 Dose to reach achievable image quality standard for 0.1 mm detail (error bars indicate 95% confidence limits).

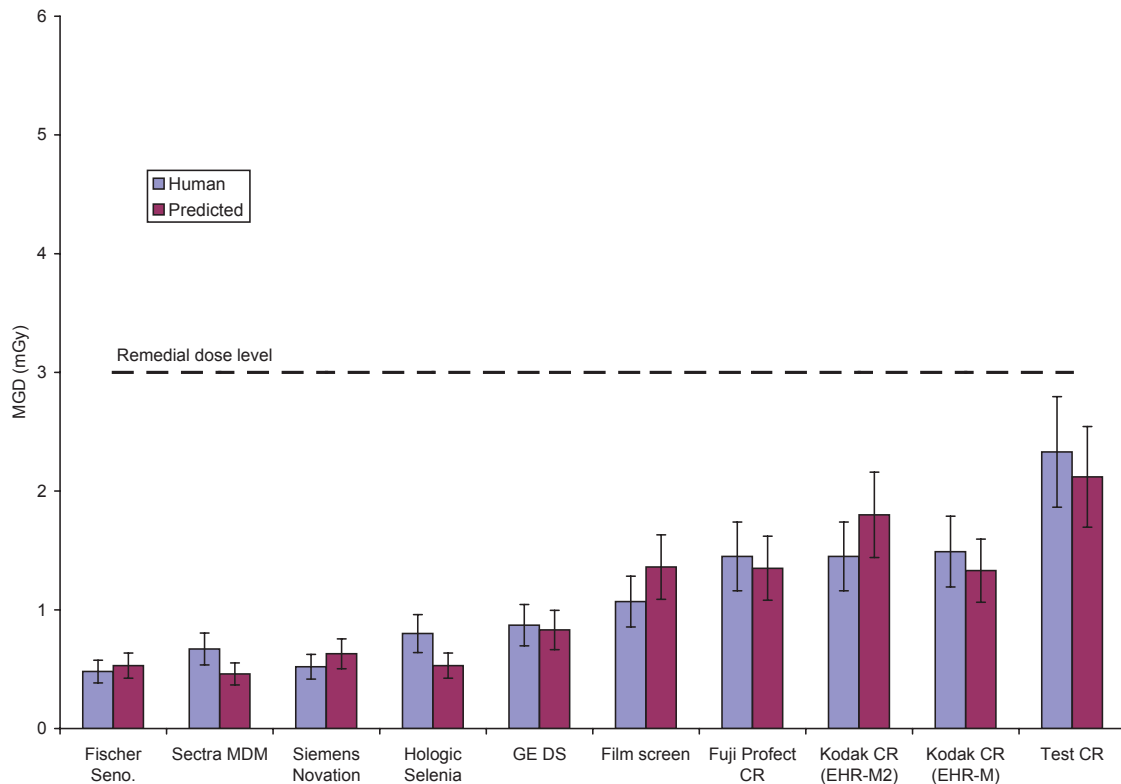


Figure 11 Dose to reach minimum image quality standard for 0.25 mm detail (error bars indicate 95% confidence limits).

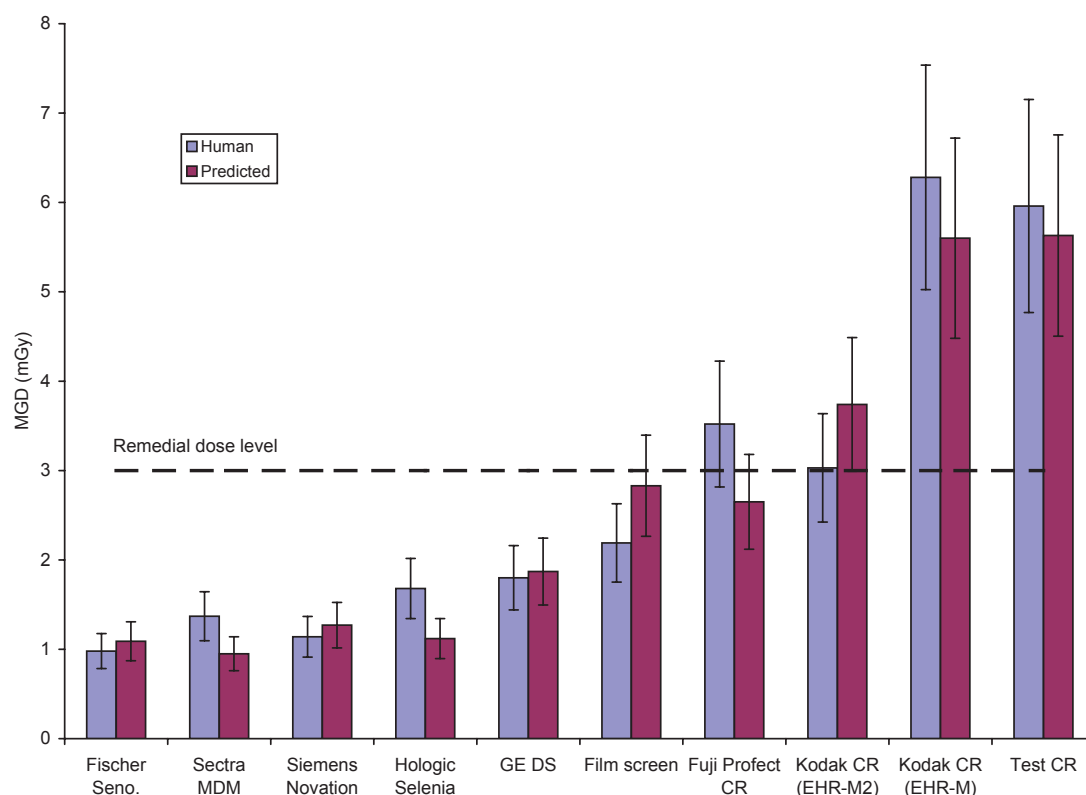


Figure 12 Dose to reach achievable image quality standard for 0.25 mm detail (error bars indicate 95% confidence limits).

3.6 Optimisation

The target CNR corresponding to the minimum image quality standard was calculated to be approximately 8.3. The MGDs required to achieve this target CNR for each beam quality and thicknesses of PMMA are shown in Figure 13. From these data the beam qualities and mAs necessary to achieve the minimum image quality standard at the lowest dose were selected and are shown in Table 8. The difference in dose between the different tube voltage and target filter combinations at the 2, 3 and 4 cm thicknesses of PMMA is very small and sometimes within measurement error. Therefore the selections shown in Table 8 at these thicknesses are given to provide representative data but some other combinations would also yield similar doses to those shown in Figure 13. At greater thicknesses of PMMA the Rh/Rh target/filter combination showed a clear advantage at all the tube voltages tested.

Table 8 Factors to achieve minimum image quality (where CNR = 8.3) at the lowest dose

PMMA thickness (mm)	kV target/filter	BGD pixel value (linearised)	mAs	MGD (mGy)	Dose compared with current AEC settings	Remedial dose level in NHSBSP protocol (mGy)
20	25 Mo/Mo	97	10	0.20	34%	1.0
30	25 Mo/Rh	96	25	0.35	45%	1.5
40	25 Rh/Rh	125	74	0.73	47%	2.0
50	25 Rh/Rh	136	163	1.38	69%	3.0
60	28 Rh/Rh	137	191	2.55	100%	4.5
70	31 Rh/Rh	140	265	4.77	123%	6.5

Technical Evaluation of the Kodak DirectView Mammography CR System

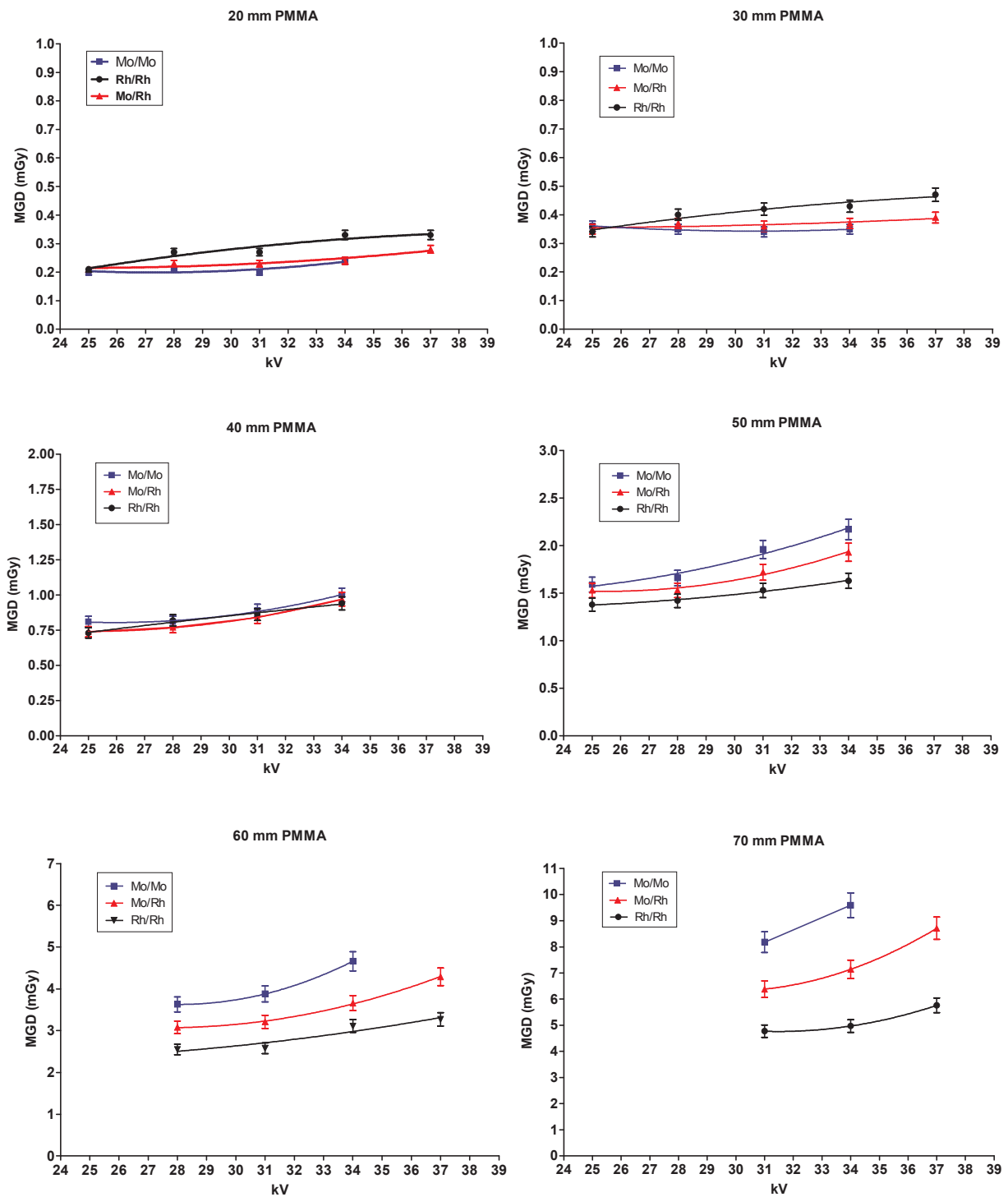


Figure 13 MGD to reach the minimum image quality standard in the NHSBSP protocol (error bars indicate 95% confidence limits).

4. DISCUSSION

The detector response was as expected non-linear with detector entrance air kerma. The noise analysis confirmed that quantum noise is the dominant noise source. The AEC resulted in doses to simulated breasts that were within the limits in the NHSBSP protocol. The dose for the standard breast simulated with 45 mm of PMMA was 1.64 mGy which is well below the upper limit of 2.5 mGy applied by the NHSBSP.

The AEC resulted in linearised pixel values that increased slowly with thickness. The AEC also chose beam qualities with higher x-ray energy with increasing thickness. The net result of these choices was that the contrast and CNR declined with increasing thickness. Comparison with the CNR necessary to reach the achievable and minimum acceptable image quality levels showed that while good image quality can be expected for breasts with small and medium thicknesses a level close to the minimum acceptable will be achieved for the largest breast thicknesses. There seems to be scope to further optimise the selection of beam qualities and dose to improve the image quality for larger breasts while keeping the dose within acceptable limits. Greater use of the Rh/Rh target/filter combination at lower thicknesses is suggested. This may be achieved by selecting 'DOSE' mode on the AEC and increasing the mAs so that the detector dose rises more steeply with increasing thickness.

The image quality measurements indicated that for the standard thickness tested (approximately equivalent to a 50 mm thickness of PMMA and 60 mm of typical breast) the image quality was slightly better than the minimum acceptable for the smallest detail size (0.1 mm). The AEC selected a dose of 2.18 mGy using 27 kV Mo/Rh. It was calculated that a dose of 2.29 ± 0.46 mGy was necessary to reach the minimum acceptable image quality level using the human readers. A similar dose of 2.34 ± 0.47 mGy was calculated to be necessary using automatic reading. At this thickness of PMMA the maximum permitted dose is 3.0 mGy. For larger detail sizes the threshold contrasts were closer to the achievable image level at the current dose selection. This difference in performance between large and small detail sizes can be explained by the relatively low MTF at high spatial frequencies which is typical of CR systems.

As is typical for a CR system the doses required to reach the acceptable and achievable image quality levels were higher than for DR systems. The results using the automated image quality assessment were broadly similar to those with human readers.

The optimisation study demonstrated that the Rh/Rh target/filter combination is preferable for breasts with a thickness equivalent to a 5 cm thickness of PMMA and above (ie ≥ 60 mm). However the use of this target filter combination will only achieve an image quality above the minimum image quality standard if the lower contrast is compensated by higher detector dose, and therefore lower detector noise. For lower breast thicknesses the doses are much lower and the choice of beam quality is less critical, but Mo/Mo or Mo/Rh are slightly preferable. The choice of kV is generally less important than the choice of target/filter combination.

5. CONCLUSIONS

Using cassettes with the new image plate design this system seems capable of producing acceptable image quality for radiation doses within the acceptable limits applied by the NHSBSP. The system met the main criteria in the NHSBSP and European protocols. As currently set up the AEC will be mostly satisfactory for most types of breast. However the system only just passes the additional criteria for AEC performance in the European protocol using 70 mm PMMA. The current adjustment of the x-ray set's AEC could be improved – especially for larger breasts. Care will be needed to ensure that each x-ray set's AEC is optimally adjusted if this system is to meet current technical requirements. A clinical evaluation for use within the NHSBSP would be appropriate. A final decision on the suitability of this system for use in the NHSBSP will depend on a review of both the technical and clinical evaluations.

REFERENCES

1. Workman A, Castellano I, Kulama E, Lawinski CP, Marshall N, Young KC. *Commissioning and Routine Testing of Full Field Digital Mammography Systems*. NHS Cancer Screening Programmes, 2006 (NHSBSP Equipment Report 0604).
2. Young KC, Johnson B, Bosmans H, Van Engen R. Development of minimum standards for image quality and dose in digital mammography. In: *Digital Mammography IWDM 2004*, Proceedings of the Workshop in Durham NC, USA, June 2004. (2005)
3. Van Engen R, Young KC, Bosmans H, Thijssen M. The European protocol for the quality control of the physical and technical aspects of mammography screening. In: *European Guidelines for Breast Cancer Screening*, 4th edition. Luxembourg: European Commission, 2006.
4. Young KC, Cook JJH, Oduko JM. Use of the European protocol to optimise a digital mammography system. In: Astley SM, Bradey M, Rose C, Zwigelaar R, editors. *Proceedings of the 8th International Workshop on Digital Mammography*. Berlin, Germany: Springer-Verlag, Lecture Notes in Computer Science, 2006, 4046: 362–369.
5. Young, KC, Oduko, JM, Bosmans H, Nijs K, Martinez L. Optimal beam quality selection in digital mammography. *British Journal of Radiology*, 2006, 79: 981–990.
6. Young, KC, Oduko, JM. *Evaluation of Kodak DirectView Mammography Computerised Radiography System*. NHS Cancer Screening Programmes, 2005 (NHSBSP Equipment Report 0504).
7. Young KC, Cook JJH, Oduko JM, Bosmans H. Comparison of software and human observers in reading images of the CDMAM test object to assess digital mammography systems. In: *Proceedings of SPIE Medical Imaging*, 2006, 614206: 1–13.
8. Young KC, Cook JJH, Oduko JM. Automated and human determination of threshold contrast for digital mammography systems. In: Astley SM, Bradey M, Rose C, Zwigelaar R, editors. *Proceedings of the 8th International Workshop on Digital Mammography*. Berlin, Germany: Springer-Verlag, Lecture Notes in Computer Science, 2006, 4046: 266–272.